SLAC – PUB – 4153
December 1986
T/E

D_s Production Data From Mark III*

WALTER TOKI
Representing the Mark III Collaboration†
Stanford Linear Accelerator Center, Stanford University, CA 94305

Abstract

Preliminary results on D_s decays from the Mark III at SPEAR are presented. The data were taken at a e^+e^- center of mass energy of $\sqrt{s} =$ 4.14 GeV with a total integrated luminosity of 6.3±0.46 pb. The decay $e^+e^- \to D_s D_s^*$, $D_s \to \phi\pi$ is observed, yielding a D_s mass of $1973 \pm 4 \pm 4$ MeV/c^2 and a D_s^* mass of $2110.8 \pm 1.9 \pm 3.2$ MeV/c^2 with a rate of $\sigma(e^+e^- \to D_s^{\pm} D_s^{*\mp},\ D_s^{*\mp} \to \gamma D_s^{\mp}) \cdot B(D_s^+ \to \phi\pi^{\pm}) = 36 \pm 7 \pm 13$ pb. There is evidence for two other modes, $D_s^{\pm} \to K^{*0}K^{\pm}$ and $D_s^{\pm} \to K_s^0 K^{\pm}$, which are observed with rates of $\sigma(e^+e^- \to D_s D_s^*) \cdot B(D_s^+ \to K^{*0}K^{\pm}) = 31$ $\pm 6 \pm 11$ pb and $\sigma(e^+e^- \to D_s D_s^*) \cdot B(D_s^{\pm} \to K_s^0 K^{\pm}) = 16 \pm 3 \pm 5$ pb.

---

* Work supported in part by the Department of Energy, under contracts DE-AC02-76ER01195, DE-AC03-76SF00515, DE-AC03-81ER40050, DE-AM03-76SF0034.

† Members of the Mark III Collaboration are D. Coffman, G. Dubois, G. Eigen, D. Hitlin, C. Matthews, Y. Zhu, *California Institute of Technology*; T. Bolton, K. O. Bunnell, R. Cassell, D. H. Coward, C. Grab, U. Mallik, R. F. Mozley, A. Odian, J. Parker, D. Pitman, R. H. Schindler, W. Stockhausen, W. Toki, F. Villa, S. Wasserbaech, D. E. Wisinski, *Stanford Linear Accelerator Center*; D. E. Dorfan, C. A. Heusch, L. Köpke, W. S. Lockman, R. Partridge, H. F. Sadrozinski, A. Seiden, M. Scarlatella, T. L. Schalk, S. Watson, A. Weinstein, R. Xu, *University of California at Santa Cruz*; G. Blaylock, J. S. Brown, B. Eisenstein, T. Freese, G. Gladding, J. Izen, C. Simopoulos, I. E. Stockdale, B. Tripsas, J. J. Thaler, A. Wattenberg, B. Wisniewski, *University of Illinois, Champaign-Urbana*; T. H. Burnett, V. Cook, A. D. Guy, R. Mir, P. Mockett, B. Nemati, L. Parrish, H. Willutzki, *University of Washington, Seattle.*

Invited talk in the Topical Conference
at the 14th SLAC Summer Institute on Particle Physics
Stanford, California, July 28-August 8, 1986

This paper presents preliminary results on D_s and D_s^* decays from the Mark III experiment at SPEAR. The data were taken in Spring 1986 at a center mass energy of $\sqrt{s} = 4.14$ GeV/c^2. This paper is divided into five sections. The first is an introduction that briefly reviews the expected D_s decay modes, the $D_s^* - D_s$ mass difference and the expected D_s production rate. The next three sections discuss separately the analyses on the three modes, $D_s^\pm \rightarrow \phi\pi^\pm$, $D_s^\pm \rightarrow K^{*0}K^\pm$ and $D_s^\pm \rightarrow K_s^0 K^\pm$ produced from $e^+e^- \rightarrow D_s D_s^*$. The last section summarizes the results.

1. Introduction

The D_s meson, a bound state of $c\bar{s}$ quarks, is expected to decay via the standard spectator diagram shown in Fig. 1a). The decay modes from this diagram include $D_s \rightarrow \phi\pi$ which has been experimentally well established.[1] Other possible diagrams are the internal W emission diagram in Fig. 1b) and the annihilation diagram in Fig.1c). The internal W emission diagram is expected to be suppressed from color counting. Some decay modes predicted from these non-spectator diagrams are $D_s \rightarrow \bar{K}^* K$ and $D_s \rightarrow \bar{K}^0 K$.

The D_s^* ,the vector partner of the pseudoscalar D_s meson, will have a slightly higher mass than the D_s. The D_s^* decay should be similar to that of the D^* except that the D_s^* should decay only via $D_s^* \rightarrow \gamma D_s$ because it has no isospin since the D_s has no u or d quarks. The simple quark model predicts a mass formula of[2]

$$m(q_1 q_2) = m_1 + m_2 \; + \; a \, \frac{\vec{s}_1 \cdot \vec{s}_2}{m_1 m_2}$$

where m_1 and m_2 are the quark masses, $\vec{s}_1$ and $\vec{s}_2$, the quark spins and a is a constant to be fitted from experimental data. This formula produces the following simple linear mass difference relation:

$$m_\rho - m_\pi = \frac{m_s}{m_u}\,(m_{K^*} - m_K) \;=\frac{m_c}{m_u}\, m_{D^*} - m_D \;= \frac{m_c m_s}{m_u^2}\,(m_{D_S^*} - m_{D_S}).$$

Using values for the quark masses of

$$m_u = m_d = .310 \text{ GeV/c}^2, \ m_s = .480 \text{ GeV/c}^2, \ m_c = 1.65 \text{ GeV/c}^2$$

yields the following predictions listed under model 1:

Mass Difference	Model 1	Model 2	Experiment
$K^* - K$	407 MeV/c^2	470 MeV/c^2	399 MeV/c^2
$D^* - D$	118 MeV/c^2	128 MeV/c^2	145 MeV/c^2
$D_s^* - D_s$	94 MeV/c^2	142 MeV/c^2	140 ? MeV/c^2

Another model predicts a mass squared difference, m^2(vector) - m^2(pseudoscalar), that is constant.[3] This difference predicts roughly equality between the difference of mass squared;

$$m_\rho^2 - m_\pi^2 = m_{K^*}^2 - m_K^2 = m_{D^*}^2 - m_D^2 = m_{D_S^*}^2 - m_{D_S}^2.$$

The results are listed under model 2. This predicts that the $D_s^* - D_s$ mass difference is very close to the $D^* - D$ mass difference or ~140 MeV/c^2.

The previous experimental data on the D_s^* comes from the TPC and ARGUS experiments.[4] The TPC group measured a D_s mass of $m_{D_S} = 1948 \pm 28 \pm 10$ MeV/c^2 and a mass difference of $m_{D_S^*} - m_{D_S} = 139.5 \pm 8.3 \pm 9.7$ MeV/c^2. The ARGUS group obtained a mass difference of $m_{D_S^*} - m_{D_S} = 144 \pm 9 \pm 7$ MeV/c^2 using an D_s mass of $m_{D_S} = 1965 \pm 3$ MeV/c^2 .

The Mark III Collaboration took data in spring 1986 in the center mass region $\sqrt{s} \simeq 4$ GeV/c^2 to confirm the D_s^* and to search for new D_s decays. The D_s's and D_s^*'s are expected to be produced via associated production of $c\bar{s}$ and $\bar{c}s$ quarks, in the modes $e^+e^- \to D_s^\pm D_s^\mp$, $D_s^\pm D_s^{*\mp}$ and $D_s^{*\pm} D_s^{*\mp}$.

The center mass energy was chosen in order to optimize the search for the D_s^*. Assuming a D_s mass of 1970 MeV/c^2 and a D_s^* mass of 2100 MeV/c^2 the following thresholds are obtained:

Mode	$\sqrt{s}$
$D_s\,\bar{D}_s$	3.94 GeV/c^2
$D_s\,\bar{D}_s^*$	4.107 GeV/c^2
$D_s^*\,\bar{D}_s^*$	4.20 GeV/c^2

The easiest method to detect the D_s^* is in the recoil against the D_s in the $e^+e^- \rightarrow D_s\bar{D}_s^*$ mode. Therefore the center mass energy was limited to $4.107 < \sqrt{s} < 4.20$ GeV/c^2. The final choice was $\sqrt{s} = 4.14$ GeV/c^2 which is roughly in between the limits. There could be threshold effects which could enhance or reduce the rate.

The D_s production rates can be crudely estimated. The formula for the $D_s\bar{D}_s$ cross section,

$$\sigma_{D_S\bar{D}_S} = \sigma_{\mu^+\mu^-}\ 3\ \left(\frac{2}{3}\right)^2\ (.15)$$

contains the relevant factors. The $\sigma_{\mu^+\mu^-}$ is the point μ pair cross section. The factor 3 is for color. The $\frac{2}{3}$ factor is the charge of the charm quark and 0.15 factor is the probability of producing a strange quark pair from the sea. Inserting the numbers yields, $\sigma_{D_S\bar{D}_S} \cong 1$ nanobarn, at $\sqrt{s} = 4.14$ GeV/c^2. This prediction does not include any contributions from threshold effects which could be sizeable. The data run at Mark III from December 1985 to February 1986 produced a total integrated luminosity of 6.3 ± 0.46 picobarns. This would produce roughly 6,000 $D_s\bar{D}_s$ pairs. Assuming an $D_s \rightarrow \phi\pi$ branching ratio of 3%, about 360 $D_s^\pm \rightarrow \phi\pi^\pm$ events should be produced in this data.

2. Analysis of the Mode $e^+e^- \to D_sD_s^*,\ D_s \to \phi\pi$

The analysis of the mode $e^+e^- \to D_sD_s^*,\ D_s \to \phi\pi$, is performed on the full data sample at a center mass energy of $\sqrt{s} = 4.1407$ GeV/c^2 with an integrated luminosity of $6.3 \pm .46$ pb. Events were selected with the following requirements:

1) Require at least three charged tracks $(\sum_i q_i = \pm 1)$;

2) TOF identification, $t_{\text{meas}} - \frac{t_K + t_\pi}{2} > 0$;

3) ϕ mass requirement, $1.0095 < m(K^+K^-) < 1.0295$ GeV/c^2.

In the TOF requirement, t_{meas} is the measured times of the charged track and $t_K(t_\pi)$ is the predicted time of flight for a kaon (pion) hypothesis. This selects tracks that have a measured time that is closer to the predicted kaon time than to the pion time. This timing requirement is applied to both oppositely charged tracks. The K^+K^- mass distribution of pairs of tracks satisfying this selection is shown in Fig. 2. There is clear evidence for the decay mode $\phi \to K^+K^-$. The peak has a fitted mass of 1019.6 ± 0.4 MeV/c^2 which agrees with the Particle Data Group value for the ϕ mass of $1019.5 \pm .1$ MeV/c^2.

To obtain $\phi\pi$ events, oppositely charged tracks satisfying this ϕ mass requirement are combined with each other charged track in the event which is assumed to be a pion. The reconstructed mass is plotted versus its recoil mass in Fig. 3. There is a cluster of events near a $\phi\pi$ mass of 1.97 GeV/c^2 and a recoil mass of 2.1 GeV/c^2. Projecting the recoil mass with a requirement that the reconstructed mass $1.925 < m(\phi\pi) < 2.025$ GeV/c^2, yields clear evidence for a D_s^* near 2.1 GeV/c^2 as shown in Fig. 4. The projection of the converse plot of the $\phi\pi$ mass with requirements that the recoil mass $2.05 < m(\text{recoil}) < 2.025$, and $1.97 < m(\text{recoil}) < 2.05$ GeV/c^2 are shown in Fig. 5a) and 5b). The former requirement selects the D^* in the recoil from the reaction $e^+e^- \to DD^*$ and in Fig. 5a) a clear D peak appears at $m_{\phi\pi} = 1854 \pm 9 \pm 7$ MeV/c^2. The latter requirement selects the D_s^* from the reaction $e^+e^- \to D_sD_s^*$ and in Fig. 5b) a clear D_s signal appears with a fitted mass of $1973 \pm 4 \pm 4$ MeV/c^2.

The $\cos\theta$ angle of the K^+ with respect to the direct of the ϕ is plotted in Fig. 6. The shape is consistent with $\cos\theta^2$ as expected for a pseudoscalar D_s decaying into $\phi\pi$, $\phi \to K^+K^-$.

To obtain a precise D_s^* mass, constraints are applied to the D_s^* mass calculation, assuming $e^+e^- \to D_s D_s^*$. The D_s^* mass is calculated as

$$m_{D_S^*} = \sqrt{E_{D_S^*}^2 - p_{D_S^*}^2}$$

$$m_{D_S^*} = \sqrt{(\sqrt{s} - E_{D_S})^2 - p_{D_S}^2}$$

$$m_{D_S^*} = \sqrt{(\sqrt{s} - \sqrt{m_{D_S}^2 + p_{D_S}^2})^2 - p_{D_S}^2}$$

where $E_{D_S(D_S^*)}$ and $p_{D_S(D_S^*)}$ are the energy and momentum of the $D_S(D_S^*)$. The constraint is applied by fixing the $\sqrt{s}$ and m_{D_S} to known values. The world average of 1970.5±2.5 MeV/c^2 is used for the D_s mass in the constraint. The only measured parameter that enters in the calculation is the momentum of the D_s. The errors in the D_s^* mass and the $D_s^* - D_s$ mass difference that are produced from the uncertainties of the D_s mass are,

$$\delta m_{D_S^*} \cong -\delta m_{D_S}$$

$$\delta\,(m_{D_S^*} - m_{D_S}) \cong -2\,\delta\, m_{D_S}.$$

The mass difference error has a factor 2 larger error than the D_s^* mass error. The constrained mass of the D_s^* is shown in Fig. 7. The constrained recoil mass distribution is a superposition of 1) the recoil mass against the D_s produced with the D_s^* in the decay process $e^+e^- \to D_s D_s^*$, and 2) the recoil mass against the D_s which decays from the D_s^* in the decay process $e^+e^- \to D_s D_s^*$, $D_s^* \to \gamma\, D_s$. The Monte Carlo simulation of the former process produces a narrow peak near 2.11 GeV/c^2 and the latter process produces a curve with a box like shape from 2.05 to 2.15 GeV/c^2. The background obtained from mixing random data events and this produces a flat distribution. These curves and their sum are shown in Fig. 7.

The D_s^* mass is determined by a maximum likelihood fit. The mass of the D_s^* is allowed to vary but the shape of the curve as determined by the Monte Carlo simulation is fixed. The fitted D_s^* mass is

$$m_{D_s^*} = (2110.8 \pm 1.9 \pm 3.2)\ \mathrm{MeV/c^2}.$$

The first error is from the fit. The second error is the systematic error which includes the error in varying the cuts of 1.6 MeV/c^2, the uncertainty in the center mass energy $\sqrt{s}$ of 1.2 MeV/c^2 and the error of the D_s mass of 2.5 MeV/c^2. This result is consistent with the previous experimental measurements of the D_s and D_s^* masses. The result supports the theoretical models which predict a constant mass squared difference.

The production rate of the D_s is obtained by fitting the number of events in Fig. 5b) with a maximum likelihood fit to a Gaussian plus a background shape. The background shape is determined from a mass distribution created by randomly combining ϕ's of one event with π's in another event. The total number of fitted events is 29.4 ± 5.4. The detection efficiency is 6.3%. The resulting cross section is

$$\sigma(e^+e^- \to D_s^\pm D_s^{*\mp}) \cdot B(D_s^\pm \to \phi\pi^\pm) = (36 \pm 7 \pm 13)\ \mathrm{pb}.$$

If the $D_s\bar{D}_s$ production rate is 1 nanobarn as estimated in the previous section the branching ratio for $D_s \to \phi\pi$ is roughly

$$B(D_s^\pm \to \phi\pi^\pm) \cong 4\%.$$

This is in good agreement with previous measurements.

3. $D_s^+ \to K^{*0}K^+$ Analysis

This analysis exploits the knowledge of the D_s^* mass by applying it as a constraint to improve the mass resolution and reject background. The following requirements are applied to the data:

1) Require at least three charged tracks $(\sum_i q_i = \pm 1)$;

2) Apply 1-C fit to, $e^+e^- \to D_s^*\ K^+K^-\pi^\pm$, where the D_s^* is not measured but the D_s^* mass constraint is applied at m=2110.8 MeV/c^2;

3) Require the TOF identification for the kaons as described in the previous section;

4) Apply a K^* mass requirement $.79 < m(K\pi) < .99$ GeV/c^2;

5) Apply a $\cos\theta_K$ requirement of $|\cos\theta_K| > 0.5$.

After applying requirements 1-3, the resulting $K\pi$ mass distribution is shown in Fig. 8. There is a clear K^{*0} peak. The fitted values are $m = 896 \pm 4$ MeV/c^2 and $\Gamma = 28 \pm 19$ MeV/c^2 which agree with Particle Data Group values of, $m_{K^{*0}} = 892 \pm 0.3$ MeV/c^2 and $\Gamma_{K^*} = 51 \pm 0.8$ MeV/c^2. To improve the signal to background ratio an additional requirement is applied on the angular distribution of the charged kaon in the rest frame of the K^{*0}. The theoretical angular distribution is $\cos^2\theta$. Requiring $|\cos\theta_K| > 0.5$ reduces the signal by 12% and the background by 50%. The resulting $K^{*0}K^\pm$ mass distribution is shown in Fig. 9. There is a clear peak near 1.97 GeV/c^2. A background distribution of the $K^+K^-\pi^\pm$ mass is obtained with a $K\pi$ requirement of $.75 < m(K^\pm\pi^\mp) < .80$ and $1.0 < m(K^\pm\pi^\mp) < 1.05$. as shown in Fig. 10. This is fitted with a polynominal and subtracted from the events in Fig. 9 to produce the background substracted plot shown Fig. 11. Fitting the peak with a Gaussian results in 24 events. The Monte Carlo efficiency is 9.75%. The resulting branching ratio is

$$\sigma(e^+e^- \to D_sD_s^*) \cdot B(D_s^\pm \to K^{*0}K^\pm) = 31 \pm 6 \pm 11 \text{ pb} .$$

Several checks have been performed. The same analysis technique is applied to detect the $D_s \to \phi\pi$ events. Taking the same events produced in this analysis, the K^+K^- mass is plotted versus the $K^+K^-\pi^\pm$ masses shown in Fig. 12. There is a clear cluster of events near the ϕ mass and the D_s mass. The $K^+K^-\pi$ mass distribution with the ϕ mass requirement around the K^+K^- mass is shown in Fig. 13. There is a clear D_s peak demonstrating the effectiveness of this method.

Another check for feed down from other processes is performed by reconstructing Monte Carlo events of the processes, $e^+e^- \to D\bar{D}^*$ and $e^+e^- \to D^*\bar{D}^*$ which are expected to be produced. Generating the expected number of events, including the known D decay modes, and applying the same analysis requirements results in the $K^+K^-\pi^\pm$ mass distribution of the expected background from D decays. No spurious D_s peak is created in these processes.

4. $D_s^+ \rightarrow K_s^0 K^+$ Analysis

The $D_s^+ \rightarrow K_s^0 K^+$ analysis is similar to that of the previous section. The analysis steps are listed below.

1) Require at least three charged tracks $(\sum_i q_i = \pm 1)$;

2) Reconstruct all oppositely charged tracks using the vector momentum at intersection of the tracks in the x-y plane and require the charged mass pair to satisfy $447 < m(\pi^+\pi^-) < 547$ MeV/c^2;

3) Require kaon TOF identification as described in the previous section for the third track;

4) Fit (2-C) the events to $e^+e^- \rightarrow D_s^* K_s^0 K^\pm$, where the D_s^* is not measured and the mass constraints of the D_s^* (m=2110.8 MeV/c^2) and K_s^0 are imposed;

5) Require the decay vertex of the K_s^0 to have a positive decay length.

The reconstructed $\pi^+\pi^-$ mass distribution is shown in Fig. 14. The mass and resolution are $476.6 \pm .12$ and $5.2 \pm .13$ MeV/c^2. The decay length is calculated imposing the direction of the K_s^0 relative to the beam as a constraint and is required to have a positive decay length. This reduces the the non-K_s^0 background. The 2-C fit to $e^+e^- \rightarrow D_s^* K_s^0 K^\pm$ where the D_s^* and K_s^0 masses are constrained improves the resolution on the $K_s^0 K^+$ mass.

The $K_s^0 K^+$ mass distribution is shown in Fig. 15. There is evidence for a signal at 1.97 GeV/c^2. The background is smoothly varying to zero. The peak contains 32 events. The Monte Carlo efficiency is .16. The resulting cross section is

$$\sigma(e^+e^- \rightarrow D_s^* D_s) \cdot B(D_s^+ \rightarrow K_s^0 K^+) = 16 \pm 3 \pm 5 \text{ pb.}$$

Several checks were performed on the data. The data was subjected to the same analysis except fit to $e^+e^- \rightarrow D^{*\pm} K_s^0 K^\mp$. This should detect the decay $D^+ \rightarrow K_s^0 K^+$. A small D^+ signal is observed near 1870 MeV/c^2 as expected.

To check that the signal is not due to $D_s^\pm \to \pi^+\pi^-K^\pm$, the analysis was redone with the K_s^0 mass constraint changed from $m = 497.7$ MeV/c^2 to 397.7 MeV/c^2 and 597.7 MeV/c^2. No D_s signal is observed from this process.

To demonstrate that the D_s signal is not due to feed down from D^* decays in the data, Monte Carlo events of $e^+e^- \to D^*\bar{D}$ and $D^*\bar{D}^*$ events were generated and reconstructed. These events were analysed with the same requirements. There is little spurious D_s signals produced in these events.

5. Summary

In conclusion, associated $D_sD_s^*$ production via the $D_s \to \phi\pi$ decay mode has been observed at $\sqrt{s} = 4.14$ GeV/c^2. The D_s^* mass was measured to be

$$m_{D_s^*} = 2110.8 \pm 1.9 \pm 3.2 \text{ MeV/c}^2.$$

There is evidence for the decay modes $D_s^\mp \to K^{*0}K^\pm$ and $K_s^0K^+$ modes. This is the first observation of the latter mode.

The preliminary branching ratios for these decays at $\sqrt{s} = 4.14$ GeV/c^2 are

$$\sigma(e^+e^- \to D_sD_s^*)\cdot B(D_s^\pm \to \phi\pi^\pm) = 36 \pm 7 \pm 13 \text{ pb;}$$

$$\sigma(e^+e^- \to D_sD_s^*)\cdot B(D_s^\pm \to K^{*0}K^\pm) = 31 \pm 6 \pm 11 \text{ pb;}$$

$$\sigma(e^+e^- \to D_sD_s^*)\cdot B(D_s^\pm \to K_s^0K^\pm) = 16 \pm 3 \pm 5 \text{ pb.}$$

In the future more analysis remains to be done with his new data from Mark III. This two body decay will allow a spin-parity test of the D_s and the D_s^*. The search will be extended to more modes. This includes the $\eta\pi$ and $\rho\pi$ modes. The total number D_s events (83 at present) may be increased in order to attempt a semileptonic measurement of the D_s and to measure the absolute branching ratios of D_s decays.

References

1. M. Aguilar–Benitez *et al.*, Phys. Lett. **170 B**, 146 (1986).
2. A simple model is described in F. Halzen and A. Martin, *Leptons and Quarks,* Wiley, New York, p. 63-66.
3. M. Frank and P. O'Donnell, Phys. Lett. **159 B**, 174 (1985).
4. H. Aihara *et al.*, Phys. Rev. Lett. **53**, 2465 (1984),
   H. Albrecht *et al.*, Phys. Lett. **146 B**, 111 (1984).

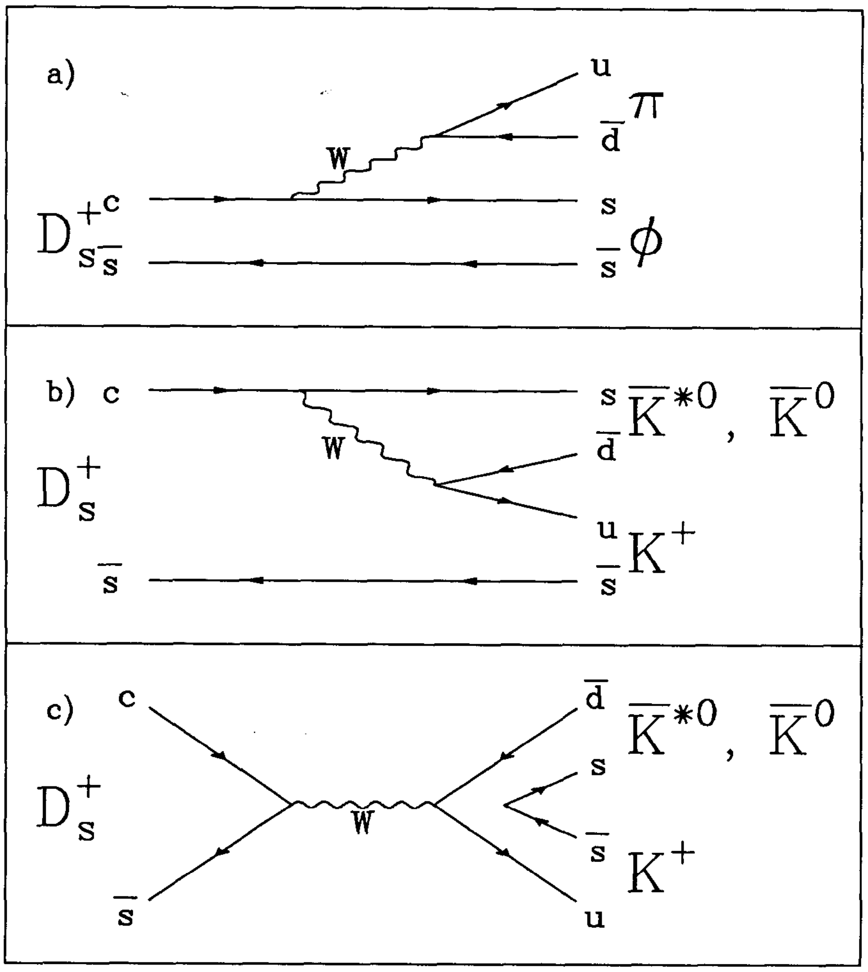

Fig. 1 D_s Weak decay diagrams

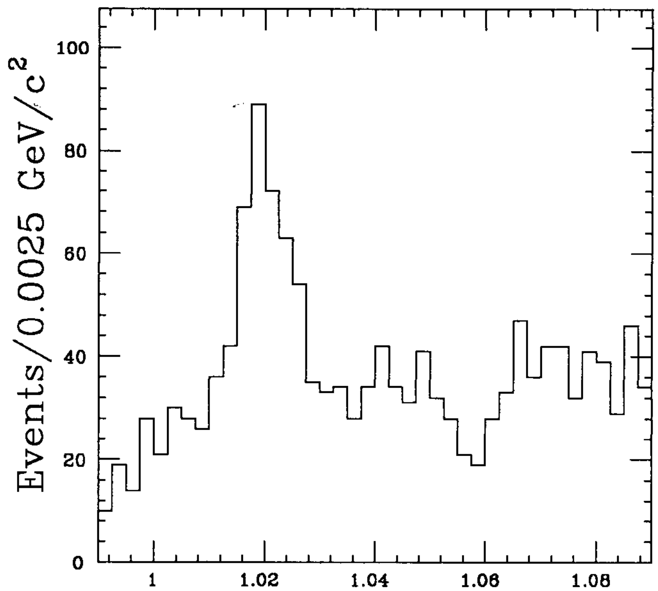

Fig. 2 K^+K^- invariant mass distribution

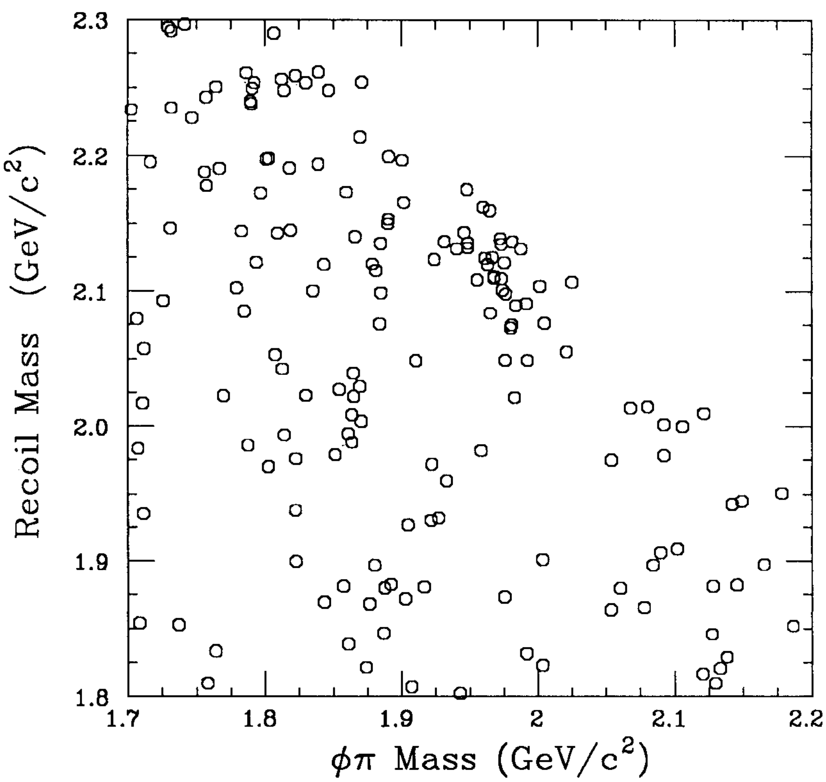

Fig. 3 Scatter Plot of $\phi\pi$ mass versus recoil mass

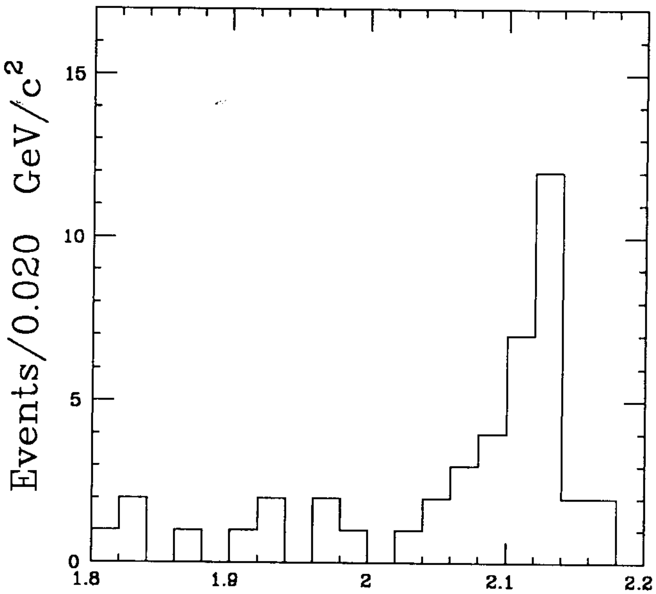

Fig. 4 Recoil mass distribution

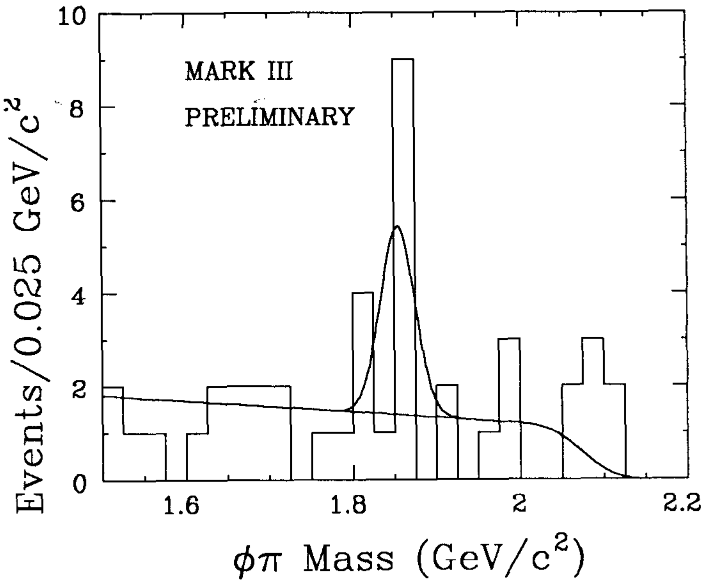

Fig. 5a $\phi\pi$ mass distribution with D requirement

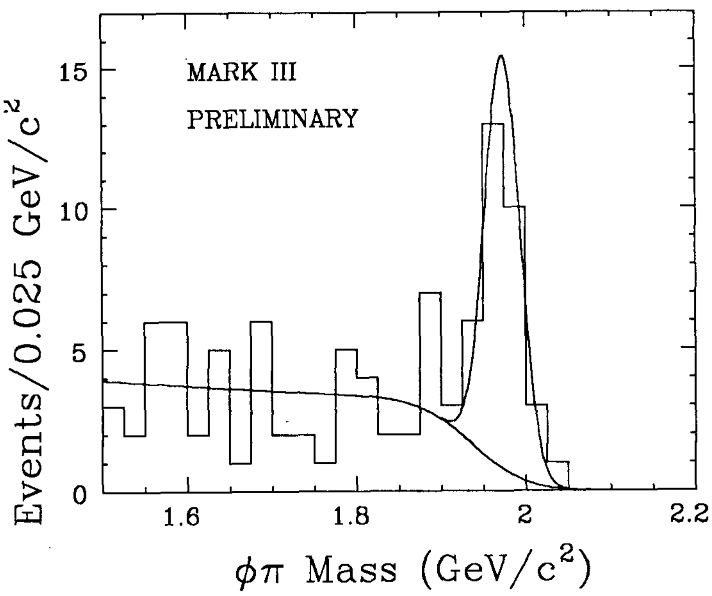

Fig. 5b $\phi\pi$ mass distribution with D_s^* requirement

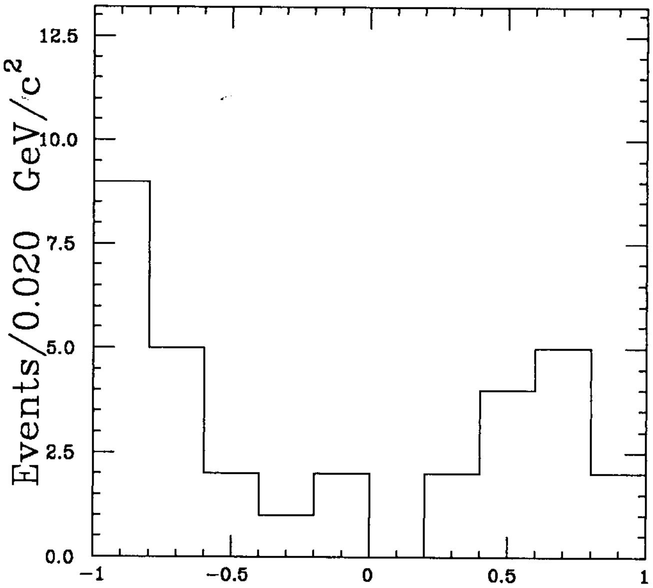

Fig. 6 $\cos\theta_K$ distribution

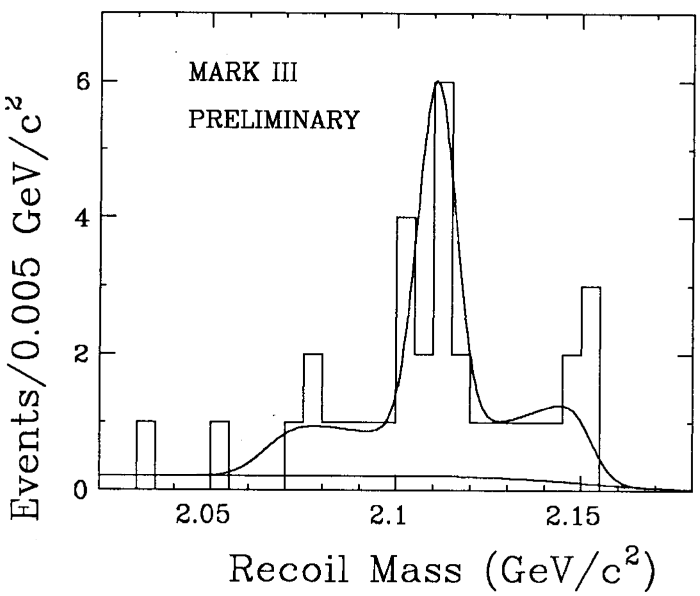

Fig. 7 Constrained Recoil Mass distribution

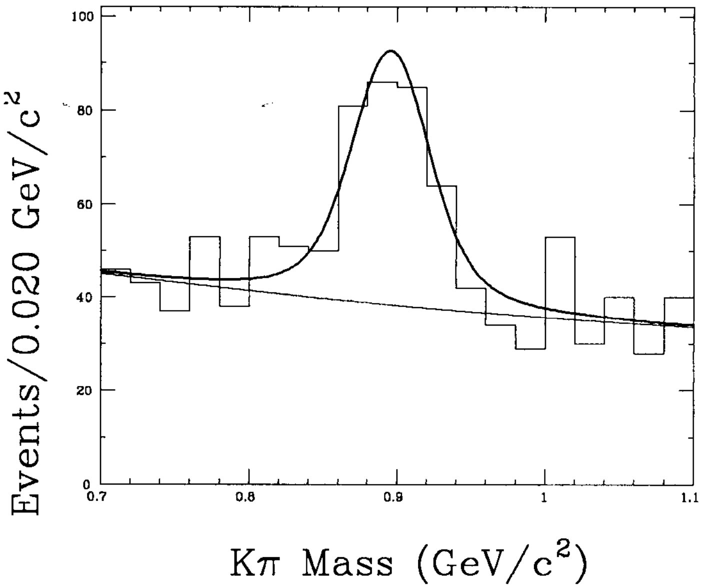

Fig. 8. $K\pi$ invariant mass distribution

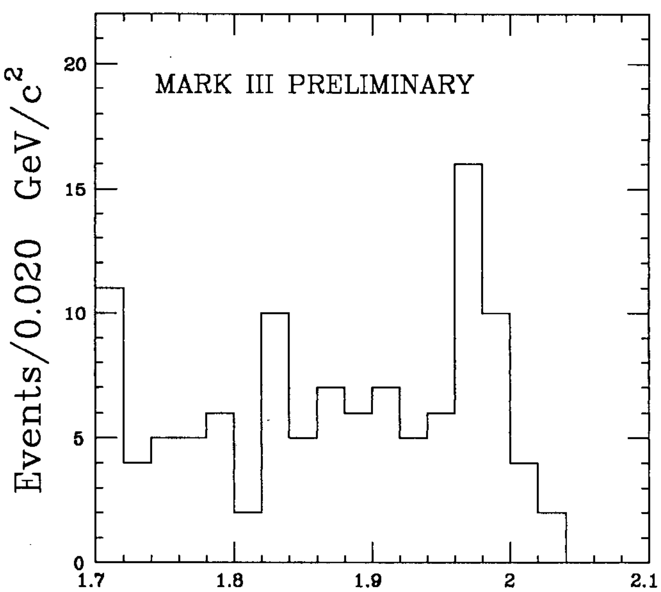

Fig. 9. $K^{*0}K$ invariant mass distribution

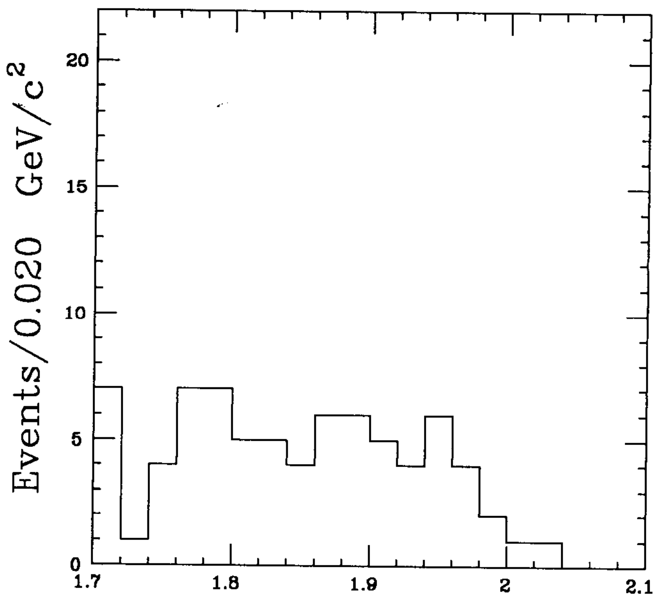

Fig. 10. $K^{*0}K$ background mass distribution

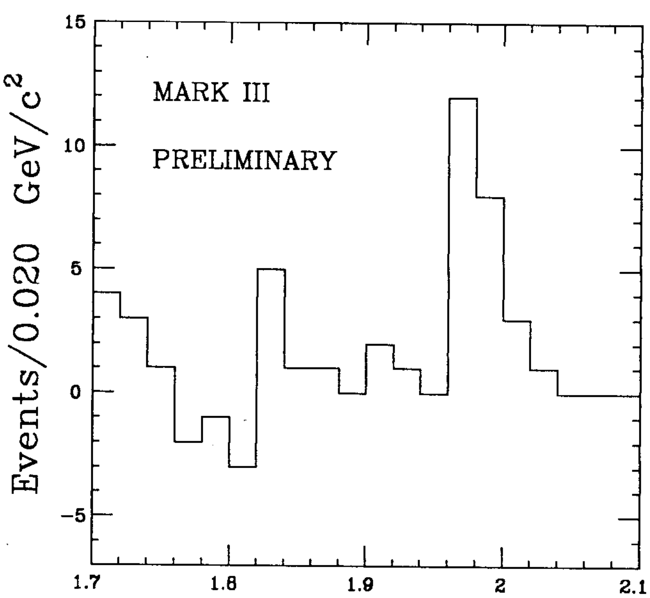

Fig. 11. $K^{*0}K$ background subtracted mass distribution

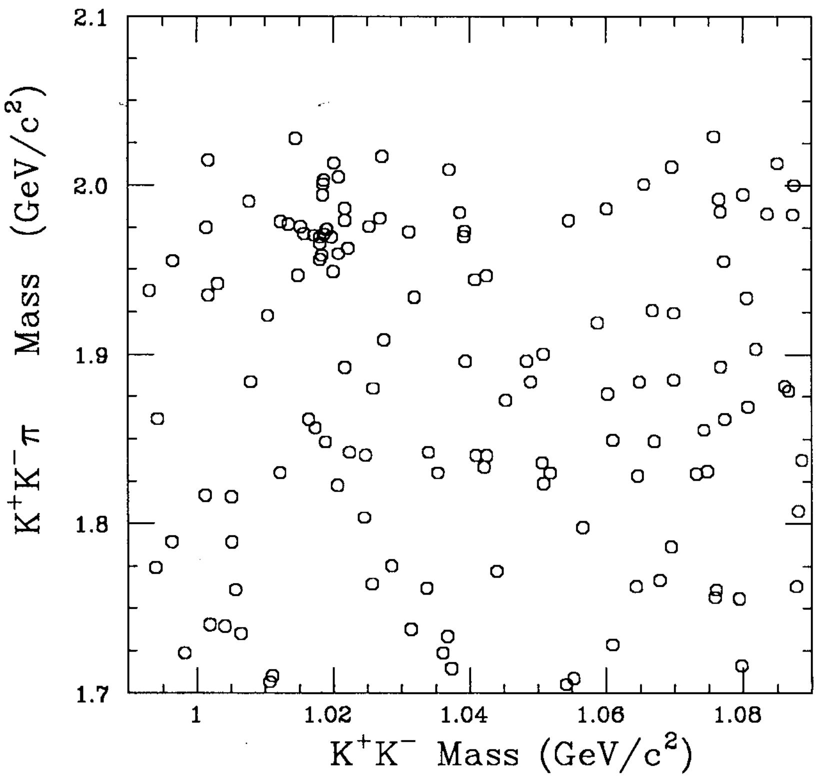

Fig. 12. K^+K^- mass versus $K^+K^-\pi$ mass

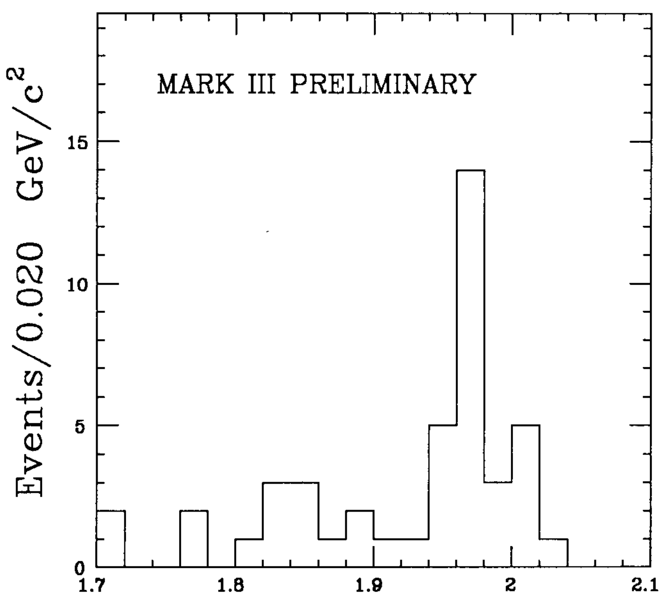

Fig. 13. $\phi\pi$ invariant mass distribution

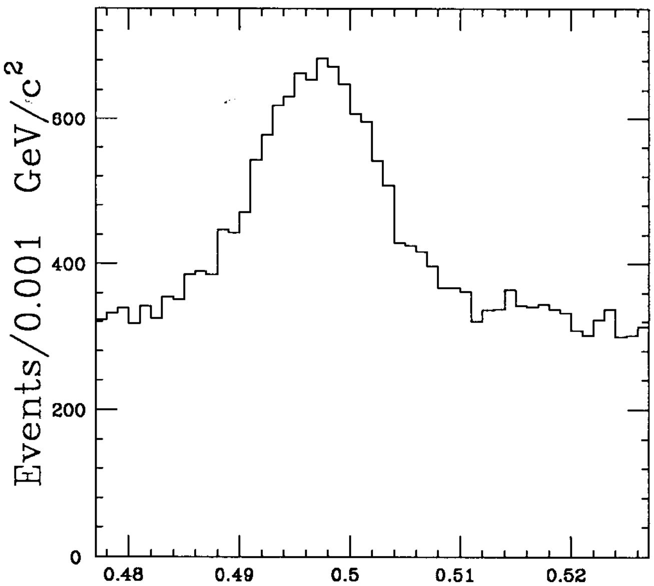

Fig. 14. $\pi^+\pi^-$ mass distribution

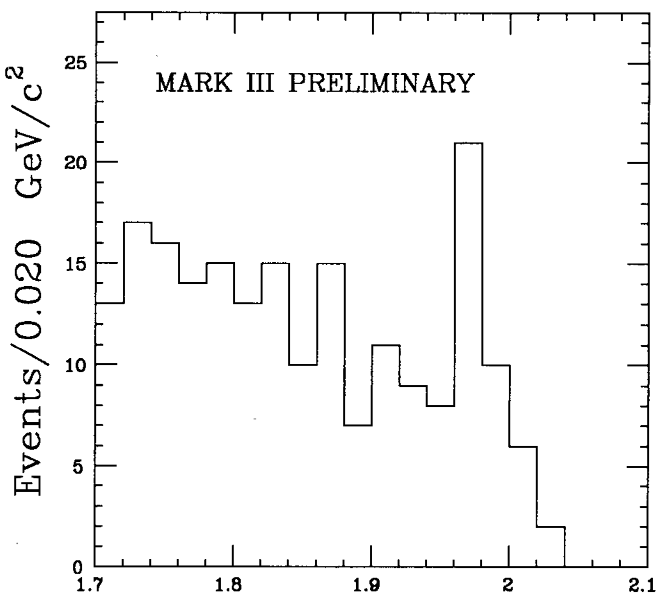

Fig. 15. $K^0K^\pm$ mass distribution